First Scan Search for Dark Photon Dark Matter with a Tunable Superconducting Radio-Frequency Cavity

Zhenxing Tang,[1,2,*] Bo Wang,[3,*] Yifan Chen,[4] Yanjie Zeng,[5,6] Chunlong Li,[5] Yuting Yang,[5,6] Liwen Feng,[1,7] Peng Sha,[8,9,10] Zhenghui Mi,[8,9,10] Weimin Pan,[8,9,10] Tianzong Zhang,[1] Yirong Jin,[11] Jiankui Hao,[1,7] Lin Lin,[1,7] Fang Wang,[1,7] Huamu Xie,[1,7] Senlin Huang,[1,7] and Jing Shu[1,2,12,†]

(SHANHE Collaboration)

[1]*School of Physics and State Key Laboratory of Nuclear Physics and Technology, Peking University, Beijing 100871, China*
[2]*Beijing Laser Acceleration Innovation Center, Huairou, Beijing 101400, China*
[3]*International Centre for Theoretical Physics Asia-Pacific, University of Chinese Academy of Sciences, 100190 Beijing, China*
[4]*Niels Bohr International Academy, Niels Bohr Institute, Blegdamsvej 17, 2100 Copenhagen, Denmark*
[5]*CAS Key Laboratory of Theoretical Physics, Institute of Theoretical Physics, Chinese Academy of Sciences, Beijing 100190, China*
[6]*School of Physical Sciences, University of Chinese Academy of Sciences, No. 19A Yuquan Road, Beijing 100049, China*
[7]*Institute of Heavy Ion Physics, Peking University, Beijing 100871, China*
[8]*Institute of High Energy Physics, Chinese Academy of Sciences, Beijing 100049, China*
[9]*Key Laboratory of Particle Acceleration Physics and Technology, Chinese Academy of Sciences, Beijing 100049, China*
[10]*Center for Superconducting RF and Cryogenics, Institute of High Energy Physics, Chinese Academy of Sciences, Beijing 100049, China*
[11]*Beijing Academy of Quantum Information Sciences, Beijing 100193, China*
[12]*Center for High Energy Physics, Peking University, Beijing 100871, China*

(Received 28 June 2023; revised 5 April 2024; accepted 29 April 2024; published 12 July 2024)

Dark photons have emerged as promising candidates for dark matter, and their search is a top priority in particle physics, astrophysics, and cosmology. We report the first use of a tunable niobium superconducting radio-frequency cavity for a scan search of dark photon dark matter with innovative data analysis techniques. We mechanically adjusted the resonant frequency of a cavity submerged in liquid helium at a temperature of 2 K, and scanned the dark photon mass over a frequency range of 1.37 MHz centered at 1.3 GHz. Our study leveraged the superconducting radio-frequency cavity's remarkably high quality factors of approximately 10^{10}, resulting in the most stringent constraints to date on a substantial portion of the exclusion parameter space on the kinetic mixing coefficient ϵ between dark photons and electromagnetic photons, yielding a value of $\epsilon < 2.2 \times 10^{-16}$.

DOI: 10.1103/PhysRevLett.133.021005

Introduction.—The quest for new physics in fundamental research has required increasingly precise measurements in recent years, specifically in detecting feeble signals from dark matter, whose existence is of utmost importance in understanding the structure and evolution of the Universe. Ultralight bosons, such as axions [1–3] and dark photons [4,5], which are predicted in many extra dimension or string-inspired models [6–9], have become notable examples of such candidates. A dark photon, a hypothetical particle from beyond the standard model of particle physics, serves as the hidden gauge boson of a U(1) interaction. Through a small kinetic mixing, dark photons can interact with ordinary photons, thus providing one of the simplest extensions to the standard model.

The detection of ultralight dark photon dark matter (DPDM) capitalizes on the tiny kinematic mixing, which contributes to weak localized effective electric currents and enables experimental probing of these elusive particles. Various search techniques for DPDM have been employed, such as dish antennas [10–12], geomagnetic fields [13,14], atomic spectroscopy [15], radio telescopes [16], and atomic magnetometers [17]. Additionally, due to similarities with axion detection [18–22], axion-photon coupling constraints have been reinterpreted to set bounds on the kinetic mixing coefficient of dark photons [23,24].

Haloscopes serve as a crucial tool for detecting ultralight dark matter. In these devices, the ultralight dark matter field is converted into electromagnetic signals within a cavity. The ongoing rapid advancements in quantum technology are anticipated to significantly bolster the sensitivity of these experimental setups [25–35]. Superconducting radio-frequency (SRF) cavities in accelerators [36] boast exceptionally high quality factors, reaching $Q_0 > 10^{10}$, allowing for the accumulation of larger electromagnetic signals and reduced noise levels [34,35,37,38]. Unlike axion detection, DPDM detection does not require a magnetic field background, enabling the full potential of superconducting cavities to be exploited. Notably, the sensitivity to the kinetic mixing coefficient of the dark photon can experience enhancement by a factor of $Q_0^{-1/4}$ in scenarios where $Q_0 > Q_{\mathrm{DM}}$ [37]. Here, $Q_{\mathrm{DM}} \approx 10^6$ characterizes the frequency spectrum of ultralight bosonic fields originating from a virialized velocity dispersion of $\sim 10^{-3}$ c.

Exploring the extensive and as yet unexplored domain within the DPDM parameter space necessitates a detector capable of systematically scanning the mass window. This imperative calls for the incorporation of a frequency tuning structure, which marks an advancement over prior investigations focused on individual bins [34,35,37]. An SRF tuning structure was recently employed in a "light-shining-through-wall" experiment for conducting broadband searches concerning dark photons [38]. In this study, for the first time, we conducted scan searches for DPDM by mechanically tuning the SRF cavity. Furthermore, a novel data analysis strategy tailored for the $Q_0 > Q_{\mathrm{DM}}$ regime was employed. This approach allowed us to access the deepest region of DPDM interaction across a majority of the scanned mass window, covering a total span of 1.37 MHz centered around a resonant frequency of 1.3 GHz. This effort represents the inaugural run of the Superconducting cavity as High-frequency gravitational wave, Axion, and other New Hidden particle Explorer (SHANHE) collaboration.

II. A tunable SRF cavity for dark photon dark matter.—Dark photon field, denoted as A'_μ, can kinetically mix with the electromagnetic photon A_μ with a form $\epsilon F'_{\mu\nu}F^{\mu\nu}/2$, where ϵ is the kinetic mixing coefficient, and $F'_{\mu\nu}$, $F^{\mu\nu}$ are the corresponding field tensors. When a coherently oscillating DPDM field is present within a cavity, it generates an effective current denoted as $\vec{J}_{\mathrm{eff}} = \epsilon m_{A'}^2 \vec{A}'$ that pumps cavity modes, where $m_{A'}$ is the dark photon mass. The DPDM field consists of an ensemble sum of nonrelativistic vector waves, with frequencies distributed in a narrow window approximately equal to $m_{A'}/(2\pi Q_{\mathrm{DM}})$ centered around $m_{A'}/(2\pi)$.

If the resonant frequency f_0 of a cavity mode falls within the frequency band around $m_{A'}/(2\pi)$, excitation of the electromagnetic field in that mode occurs, resulting in a signal power proportional to $\epsilon^2 m_{A'} V C \rho_{A'}$, where V is the cavity volume, C is the form factor that characterizes the overlap between a cavity mode and the DPDM wave function along a specific axis (see Supplemental Material for detail [39]), and $\rho_{A'} \approx 0.45\ \mathrm{GeV/cm^3}$ is the local dark matter energy density. On the other hand, both internal dissipation of the cavity and amplifiers introduce noise, $P_n = P_{\mathrm{th}} + P_{\mathrm{amp}}$. P_{th} represents the power of thermal noise in the cavity and is proportional to $T f_0/Q_0$, where T is the temperature of the cavity. The signal and thermal noise are distributed within the same bandwidth $\approx (\beta+1) f_0/Q_0$ in the limit that the cavity's quality factor Q_0 is much greater than Q_{DM}. Here, β is the dimensionless cavity coupling factor representing the ratio between the power transferred to the readout port and the internal dissipation. The noise from the amplifier is characterized by its effective noise temperature T_{amp}. The spectrum of the amplifier noise is flat within a frequency range Δf_0, which is the range over which the cavity's resonant frequency can be kept stable. Consequently, the amplifier noise dominates over the thermal noise when $T_{\mathrm{amp}} \approx T$.

The signal-to-noise ratio (SNR) of each scan step's search can be estimated by using the Dicke radiometer equation: $\mathrm{SNR} = \sqrt{t_{\mathrm{int}} \Delta f_0} P_{\mathrm{sig}}/P_n$ [48], where t_{int} denotes the integration time. This estimation enables us to determine the level of sensitivity toward ϵ,

$$\epsilon \approx 2.8 \times 10^{-16} \left(\frac{10^{10}}{Q_0}\right)^{\frac{1}{4}} \left(\frac{\xi}{100}\right)^{\frac{1}{4}} \left(\frac{4\mathrm{L}}{V}\right)^{\frac{1}{2}} \left(\frac{0.5}{C}\right)^{\frac{1}{2}} \left(\frac{100\ \mathrm{s}}{t_{\mathrm{int}}}\right)^{\frac{1}{4}} \left(\frac{1.3\ \mathrm{GHz}}{f_0}\right)^{\frac{1}{4}} \left(\frac{T_{\mathrm{amp}}}{3\ \mathrm{K}}\right)^{\frac{1}{2}}, \tag{1}$$

where $\xi \equiv \Delta f_0 Q_0 / f_0$, and we require $\mathrm{SNR} = 1.64$, and take $\beta \approx 1$, and $T \approx T_{\mathrm{amp}}$, as calibrated in this study, and $\rho_{A'} = 0.45\ \mathrm{GeV/cm^3}$. Equation (1) shows that high quality factors improve sensitivity to ϵ, as $\epsilon \propto Q_0^{-1/4}$. SRF cavities are therefore powerful transducers for detecting DPDM [37].

In this Letter, we used a single-cell elliptical niobium SRF cavity, as illustrated in Fig. 1. The cavity has a volume $V \simeq 3.9$ L. We employ the ground mode TM_{010} at $f_0 \simeq 1.3$ GHz, resulting in a form factor of $C \simeq 0.53$. To search DPDM within a reasonable mass range, it is imperative to scan the cavity at various resonant frequencies. To achieve this, a double lever frequency tuner [49,50], as depicted in Fig. 1, was installed on the cavity. This tuner includes a stepper motor with a tuning resolution of approximately 10 Hz, and a piezo actuator capable of fine-tuning at a level of 0.1 Hz. A detailed schematic of this tuner is provided in the Supplemental Material [39]. The cavity, along with the tuning apparatus and the experimental platform, has undergone extensive testing over several years [51–56].

Experimental operation.—Before carrying out DPDM searches, it is essential to calibrate the relevant cavity and amplifier parameters. All calibrated parameters and the corresponding uncertainties are presented in Table I. Both

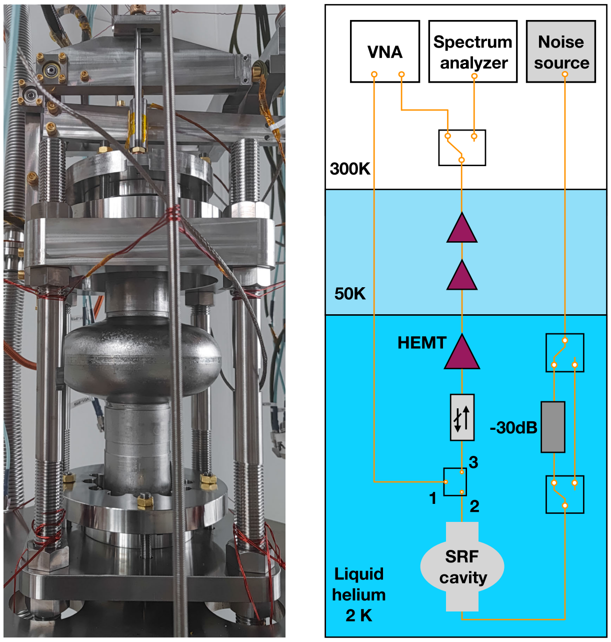

FIG. 1. Left: Single-cell SRF cavity equipped with frequency tuner. Right: Schematic of the microwave electronics for DPDM searches. The VNA measures the net amplification factor $G_{\rm net}$ of the amplifier circuit consisting of an isolator, a HEMT amplifier, and two room-temperature amplifiers. The noise source and the spectrum analyzer calibrate the resonant frequencies f_0^i. The time-domain signals from the SRF, with sequential amplification, are finally recorded by the spectrum analyzer.

the volume of the cavity and the form factor of the TM_{010} mode are calculated numerically, with $< 1\%$ uncertainty for effective volume $V_{\rm eff} \equiv VC/3$. This uncertainty originates from the slight discrepancy between the simulated resonant frequency and the experimentally measured one, along with potential effects such as thinning due to acid pickling procedures. Here, the factor of $1/3$ accounts for the random distribution of DPDM polarization.

We present the experimental setup in which the microwave electronics are depicted in the right panel of Fig. 1. The cavity is positioned within a liquid helium environment at a temperature $T \simeq 2$ K and is connected to axial pin

TABLE I. Calibrated parameters for SRF cavities and amplifiers used are shown, including their mean values, uncertainties, and fractional uncertainties on DPDM-induced power, F_j.

	Value	Fractional uncertainty
$V_{\rm eff} \equiv VC/3$	693 mL	$< 1\%$
β	0.634 ± 0.014	1.4%
$G_{\rm net}$	(57.30 ± 0.14) dB	3.1%
Q_L	$(9.092 \pm 0.081) \times 10^9$	/
$f_0^{\rm max}$	1.299 164 379 5 GHz	/
Δf_0	11.5 Hz	/
$t_{\rm int}$	100 s	/

couplers. The amplifier line consists of an isolator, which serves to prevent the injection of amplifier noise into the cavity, a high-electron mobility transistor (HEMT) amplifier, and two room-temperature amplifiers. Initially, we used a vector network analyzer (VNA) to measure the net amplification factor $G_{\rm net}$ of the amplifier circuit, which considers the sequential amplification and potential decays within the line. Next, we conducted decay measurements with a noise source that went through the cavity, the amplifier line, and the spectrum analyzer, to calibrate the cavity loaded quality factor, $Q_L \equiv Q_0/(\beta+1)$. The cavity coupling factor, β, was calibrated in combination with the results of the standard vertical test stand.

For each scan step, we used the noise source to calibrate the resonant frequency f_0 of the cavity by locating the peak of the power spectral density. This injected noise, featuring a spectrum wider than the cavity's bandwidth, serves as an effective stand-in for synthetic signals, ensuring that our data analysis procedures are well-suited for accurate signal detection. Immediately after calibration, we switched off the noise source and inserted a 30 dB attenuator to prevent the external noise from entering the cavity. We then used the spectrum analyzer to record the time-domain signals from the SRF cavity and amplifiers. Each scan took $t_{\rm int} = 100$ s. After each scan, the value of f_0 was adjusted by approximately 1.3 kHz and the calibration of f_0 was restarted. A total of $N_{\rm bin} = 1150$ scans were conducted, covering a frequency range of approximately 1.37 MHz. The highest resonant frequency, denoted by $f_0^{\rm max}$, occurred when the frequency tuner was not applied. The calibration process for $G_{\rm net}$, Q_L, and β was conducted multiple times during the whole scan process, with uncertainties given by the measurement deviation.

One key challenge of DPDM searches using SRF is to ensure any potential signal induced from DPDM is within the resonant bin, as f_0 may drift with time or oscillate due to microphonics effect [38,50]. To determine the stability range of f_0, denoted as Δf_0, we measured the drift of f_0 every 50 scans, matching the integration time $t_{\rm int}$ of a single scan step, and also assessed the effect of microphonics over the same duration (see Supplemental Material [39]). The microphonics effect produces a resonant frequency distribution with a root mean square of $\delta f_m^{\rm rms} = 4.1$ Hz, which is dominant over the drift with a maximum deviation of 1.5 Hz. To account for any potential deviations in f_0, we conservatively selected Δf_0 to be $2.8 \delta f_m^{\rm rms} \simeq 11.5$ Hz, taking into consideration an efficiency of 84% for the recorded signal to optimize the SNR.

Data analysis and constraints.—In this Letter, each scan was focused on the frequency bin centered at the resonant frequency f_0, which had a bandwidth of Δf_0. For every scan, we obtained $N = t_{\rm int} \Delta f_0$ samples at the resonant bin and computed their average value and standard deviation. We checked the Gaussian noise property by ensuring that the ratio between these two values was close to 1 at each step.

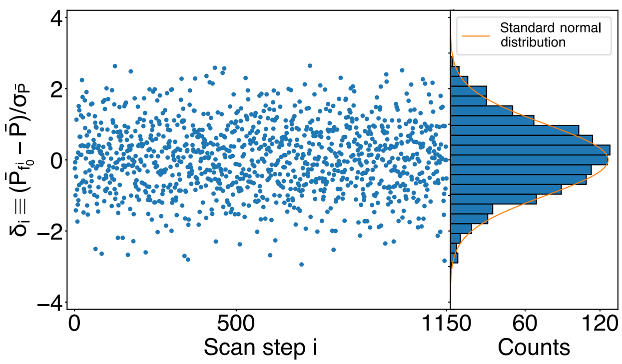

FIG. 2. The blue dots show the normalized power excess $\delta_i \equiv (\bar{P}_{f_0^i} - \bar{P})/\sigma_{\bar{P}}$ at each scan step i. Its distribution is shown on the right panel, which can be well fit by a standard normal distribution.

The average values of different scans provided an indication of the total noise in each resonant bin. The amplifier noise, P_{amp}, was found to be nearly constant over the entire frequency range tested. Furthermore, the subdominant thermal noise was observed to be linearly proportional to the resonant frequency, with a variation much smaller than the standard deviation. Therefore, we expected the noise in the resonant bins to be independent of the resonant frequency. To reduce the potential effects of environmental variation, such as helium pressure fluctuations and mechanical vibrations, we aggregated every 50 contiguous bins to ensure environmental stability within each group. For each group, we computed a constant fit for different bins and presented the normalized power excess in Fig. 2. The right panel of the figure shows a comparison between the counts of normalized power excess and the standard normal distribution to confirm its Gaussianity. No deviation over 3σ appears in any bin. Note that the scan steps do not progress in a strictly monotonic order by frequency, as continuously tuning the frequency in a single direction can induce additional drift of f_0. Monotonic progression is maintained only within groups of 50 consecutive bins.

Compared to the analysis strategies employed by traditional haloscopes with $Q_0 \ll Q_{\mathrm{DM}}$, our resonant bins cover only a fraction of the entire frequency band, $\Delta f_0 Q_{\mathrm{DM}}/f_0$. However, we can still test the DPDM with masses within this range and thereby maximize the scan rate. Furthermore, our simple fit function results in attenuation factor of 98%. This value is less suppressed when compared to low Q_0 experiments, where higher-order fitting functions are utilized to account for the frequency-dependent cavity response during each scan.

There are two sources of uncertainty that affect the sensitivity toward DPDM searches. In addition to the fit uncertainty caused by Gaussian noise, there are also uncertainties in calibrated parameters that may contribute to a biased estimate for DPDM-induced signals. We present the measurement uncertainties of parameters $V_{\mathrm{eff}}, \beta, G_{\mathrm{net}}$ and

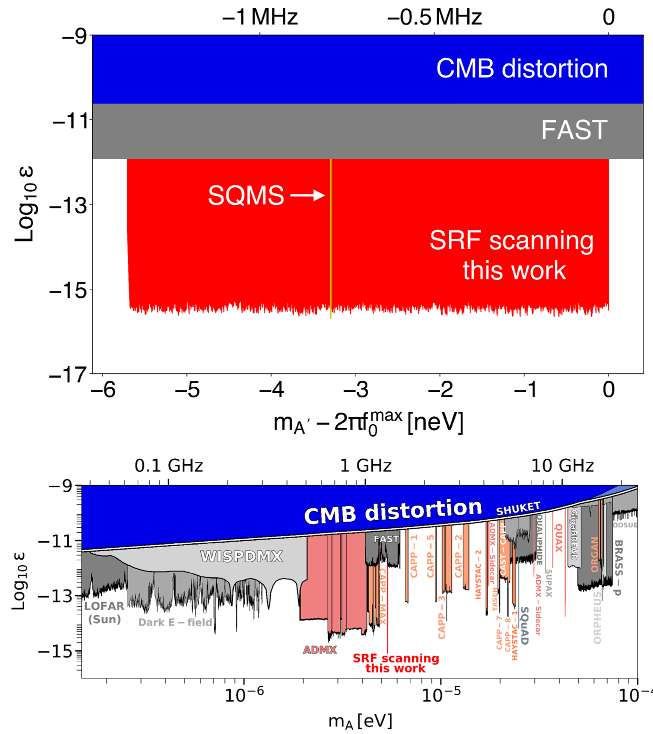

FIG. 3. Top: The 90% exclusion on the kinetic mixing coefficient ϵ of DPDM based on SRF scan searches performed in this study (red). Other constraints including FAST radio telescope (gray) [16], distortion of cosmic microwave background (blue) [5], and SQMS prototype (yellow) [37] are shown for comparison. Bottom: A comparison of our results within the broader context of existing constraints, adapted from [57].

their corresponding fractional influences on signal power in Table I (see Supplemental Material [39]). To compute the probability function for a potential DPDM signal, we multiply the contributions from different bins. However, because the DPDM width $\approx m_{A'}/(2\pi Q_{\mathrm{DM}})$ is much larger than the narrow bandwidth Δf_0, we only consider the two nearby bins in practice. Figure 3 shows the 90% upper limits on the kinetic mixing coefficient ϵ for a given DPDM mass $m_{A'}$. The high quality factor of SRF significantly boosts sensitivity, leading to the most stringent constraints compared to other limitations across a wide range of investigated masses. The reached sensitivity is well-estimated by Eq. (1). For comparative analysis, we present the outcomes of a single-bin search conducted in Superconducting Quantum Materials and Systems Center (SQMS) [37] in the top panel. Both investigations utilized a conventional 1.3 GHz elliptical cavity, yielding akin parameters encompassing V_{eff}, f_0, β, and Q_L. The primary distinction between our parameters and theirs lies in the bin size and integration time. Specifically, our t_{int} is 10 times shorter than theirs. We conservatively selected $\Delta f_0 = 11.5$ Hz, whereas their choice is only 0.15 Hz. The bottom panel presents a comparison across a wider frequency range with other experiments, clearly demonstrating that SRF experiments achieve the deepest sensitivity.

Conclusion.—In this Letter, we utilized a tunable single-cell 1.3 GHz elliptical cavity to search for DPDM. Our findings establish the most stringent exclusion limit across a majority of the scanned mass window, achieving a depth of sensitivity of up to $\epsilon \sim 2.2 \times 10^{-16}$. This result demonstrates that employing cavities with high quality factors significantly enhances the sensitivity toward the kinetic mixing coefficient of DPDM. Our experiment presents the first scan results using a tunable SRF cavity, which covers a frequency range of 1.37 MHz within DPDM's mass window, beginning from an initial resonant frequency of approximately $f_0^{\max} \simeq 1.299$ GHz. Our scan steps are set at intervals corresponding to 10^{-6} of the resonant frequency, aligning with the dark matter bandwidth to optimize the scan rate. To investigate any potential excess from a suspicious signal, we can simply adjust the resonant frequency slightly away from the bin indicating excess. Conducting a comprehensive scan of the surrounding region allows for the reconstruction of the frequency spectrum of DPDM, providing valuable insights into the mechanisms of dark matter formation.

In the upcoming phase of our DPDM search, our foremost goals are to broaden the tuning range and boost sensitivity. We are in the process of designing a new tuning mechanism—a plunger tuner—that will adjust the beam pipe's end face at one end of the cavity. This adjustment is projected to enhance the tuning range to approximately 1/10 of the resonant frequency. To further augment sensitivity, our strategy includes mitigating microphonics effects and diminishing amplifier noise, utilizing dilution refrigeration and nearly quantum-limited Josephson parametric amplifiers. Additionally, by employing coupled-cavity designs, we anticipate increasing the cavity volume tenfold while maintaining the same resonant frequency. With these advancements combined, we are optimistic about setting new constraints on the kinetic mixing coefficient ϵ, potentially below 10^{-17}.

The exceptionally high quality factors of SRF cavities open avenues for additional enhancements in detection sensitivity. For example, coupling a single cavity mode to a multimode resonant systems with nondegenerate parametric interactions [25–28] can broaden the effective bandwidth of each scan without losing sensitivity within it. One can also exploit squeezing technology [29–33] or nondemolition photon counting [34,35] to go beyond the standard quantum limit. A network of DPDM detectors simultaneously measuring at the same frequency band will not only increase the sensitivity [26,58], but also reveal macroscopic properties and the microscopic nature of the DPDM sources, such as the angular distribution and polarization [59,60].

We are grateful to Raphael Cervantes for useful discussions. We acknowledge the utilization of the Platform of Advanced Photon Source Technology R&D. This work is supported by the National Key Research and Development Program of China under Grant No. 2020YFC2201501, and by the Munich Institute for Astro-, Particle, and BioPhysics (MIAPbP), which is funded by the Deutsche Forschungsgemeinschaft (DFG, German Research Foundation) under Germany's Excellence Strategy—EXC-2094–390783311. Y. C. is supported by VILLUM FONDEN (Grant No. 37766), by the Danish Research Foundation, and under the European Union's H2020 ERC Advanced Grant "Black holes: gravitational engines of discovery" Grant Agreement No. Gravitas–101052587, and by FCT (Fundação para a Ciência e Tecnologia I.P, Portugal) under Project No. 2022.01324.PTDC. P. S. is supported by the National Natural Science Foundation of China under Grant No. 12075270. J. S. is supported by Peking University under startup Grant No. 7101302974 and the National Natural Science Foundation of China under Grants No. 12025507, No. 12150015, and is supported by the Key Research Program of Frontier Science of the Chinese Academy of Sciences (CAS) under Grant No. ZDBS-LY-7003 and CAS project for Young Scientists in Basic Research YSBR-006.

[*]These authors contributed equally to this work.
[†]Corresponding author: jshu@pku.edu.cn

[1] John Preskill, Mark B. Wise, and Frank Wilczek, Cosmology of the invisible axion, Phys. Lett. **120B**, 127 (1983).
[2] L. F. Abbott and P. Sikivie, A cosmological bound on the invisible axion, Phys. Lett. **120B**, 133 (1983).
[3] Michael Dine and Willy Fischler, The not so harmless axion, Phys. Lett. **120B**, 137 (1983).
[4] Ann E. Nelson and Jakub Scholtz, Dark light, dark matter and the misalignment mechanism, Phys. Rev. D **84**, 103501 (2011).
[5] Paola Arias, Davide Cadamuro, Mark Goodsell, Joerg Jaeckel, Javier Redondo, and Andreas Ringwald, WISPy cold dark matter, J. Cosmol. Astropart. Phys. 06 (2012) 013.
[6] Peter Svrcek and Edward Witten, Axions in string theory, J. High Energy Phys. 06 (2006) 051.
[7] S. A. Abel, M. D. Goodsell, J. Jaeckel, V. V. Khoze, and A. Ringwald, Kinetic mixing of the photon with hidden U(1)s in string phenomenology, J. High Energy Phys. 07 (2008) 124.
[8] Asimina Arvanitaki, Savas Dimopoulos, Sergei Dubovsky, Nemanja Kaloper, and John March-Russell, String axiverse, Phys. Rev. D **81**, 123530 (2010).
[9] Mark Goodsell, Joerg Jaeckel, Javier Redondo, and Andreas Ringwald, Naturally light hidden photons in LARGE volume string compactifications, J. High Energy Phys. 11 (2009) 027.
[10] Dieter Horns, Joerg Jaeckel, Axel Lindner, Andrei Lobanov, Javier Redondo, and Andreas Ringwald, Searching for WISPy cold dark matter with a dish antenna, J. Cosmol. Astropart. Phys. 04 (2013) 016.
[11] A. Andrianavalomahefa *et al.* (FUNK Experiment Collaboration), Limits from the funk experiment on the mixing strength of hidden-photon dark matter in the visible and

near-ultraviolet wavelength range, Phys. Rev. D **102**, 042001 (2020).
[12] Karthik Ramanathan, Nikita Klimovich, Ritoban Basu Thakur, Byeong Ho Eom, Henry G. LeDuc, Shibo Shu, Andrew D. Beyer, and Peter K. Day, Wideband direct detection constraints on hidden photon dark matter with the QUALIPHIDE experiment, Phys. Rev. Lett. **130**, 231001 (2023).
[13] Michael A. Fedderke, Peter W. Graham, Derek F. Jackson Kimball, and Saarik Kalia, Earth as a transducer for dark-photon dark-matter detection, Phys. Rev. D **104**, 075023 (2021).
[14] Michael A. Fedderke, Peter W. Graham, Derek F. Jackson Kimball, and Saarik Kalia, Search for dark-photon dark matter in the SuperMAG geomagnetic field dataset, Phys. Rev. D **104**, 095032 (2021).
[15] Joshua Berger and Amit Bhoonah, First laboratory bounds on ultralight dark photon dark matter from precision atomic spectroscopy, arXiv:2206.06364.
[16] Haipeng An, Shuailiang Ge, Wen-Qing Guo, Xiaoyuan Huang, Jia Liu, and Zhiyao Lu, Direct detection of dark photon dark matter using radio telescopes, Phys. Rev. Lett. **130**, 181001 (2023).
[17] Min Jiang, Taizhou Hong, Dongdong Hu, Yifan Chen, Fengwei Yang, Tao Hu, Xiaodong Yang, Jing Shu, Yue Zhao, and Xinhua Peng, Search for dark photons with synchronized quantum sensor network, Nat. Commun. **15**, 3331 (2024).
[18] P. Sikivie, Experimental tests of the invisible axion, Phys. Rev. Lett. **51**, 1415 (1983); Phys. Rev. Lett. **52**, 695(E) (1984).
[19] Pierre Sikivie, Detection rates for 'invisible' axion searches, Phys. Rev. D **32**, 2988 (1985); Phys. Rev. D **36**, 974(E) (1987).
[20] P. Sikivie, N. Sullivan, and D. B. Tanner, Proposal for axion dark matter detection using an LC circuit, Phys. Rev. Lett. **112**, 131301 (2014).
[21] Saptarshi Chaudhuri, Peter W. Graham, Kent Irwin, Jeremy Mardon, Surjeet Rajendran, and Yue Zhao, Radio for hidden-photon dark matter detection, Phys. Rev. D **92**, 075012 (2015).
[22] Yonatan Kahn, Benjamin R. Safdi, and Jesse Thaler, Broadband and resonant approaches to axion dark matter detection, Phys. Rev. Lett. **117**, 141801 (2016).
[23] Sumita Ghosh, E. P. Ruddy, Michael J. Jewell, Alexander F. Leder, and Reina H. Maruyama, Searching for dark photons with existing haloscope data, Phys. Rev. D **104**, 092016 (2021).
[24] Andrea Caputo, Alexander J. Millar, Ciaran A. J. O'Hare, and Edoardo Vitagliano, Dark photon limits: A handbook, Phys. Rev. D **104**, 095029 (2021).
[25] Xiang Li, Maxim Goryachev, Yiqiu Ma, Michael E. Tobar, Chunnong Zhao, Rana X. Adhikari, and Yanbei Chen, Broadband sensitivity improvement via coherent quantum feedback with PT symmetry, arXiv:2012.00836.
[26] Yifan Chen, Minyuan Jiang, Yiqiu Ma, Jing Shu, and Yuting Yang, Axion haloscope array with PT symmetry, Phys. Rev. Res. **4**, 023015 (2022).
[27] K. Wurtz, B. M. Brubaker, Y. Jiang, E. P. Ruddy, D. A. Palken, and K. W. Lehnert, Cavity entanglement and state swapping to accelerate the search for axion dark matter, PRX Quantum **2**, 040350 (2021).
[28] Yue Jiang, Elizabeth P. Ruddy, Kyle O. Quinlan, Maxime Malnou, Nicholas E. Frattini, and Konrad W. Lehnert, Accelerated weak signal search using mode entanglement and state swapping, PRX Quantum **4**, 020302 (2023).
[29] Huaixiu Zheng, Matti Silveri, R. T. Brierley, S. M. Girvin, and K. W. Lehnert, Accelerating dark-matter axion searches with quantum measurement technology, arXiv:1607.02529.
[30] M. Malnou, D. A. Palken, B. M. Brubaker, Leila R. Vale, Gene C. Hilton, and K. W. Lehnert, Squeezed vacuum used to accelerate the search for a weak classical signal, Phys. Rev. X **9**, 021023 (2019); Phys. Rev. X**10**, 039902(E) (2020).
[31] K. M. Backes *et al.* (HAYSTAC Collaboration), A quantum-enhanced search for dark matter axions, Nature (London) **590**, 238 (2021).
[32] K. W. Lehnert, Quantum enhanced metrology in the search for fundamental physical phenomena, SciPost Phys. Lect. Notes **40**, 1 (2022).
[33] M. J. Jewell *et al.* (HAYSTAC Collaboration), New results from HAYSTAC's phase II operation with a squeezed state receiver, Phys. Rev. D **107**, 072007 (2023).
[34] Akash V. Dixit, Srivatsan Chakram, Kevin He, Ankur Agrawal, Ravi K. Naik, David I. Schuster, and Aaron Chou, Searching for dark matter with a superconducting qubit, Phys. Rev. Lett. **126**, 141302 (2021).
[35] Ankur Agrawal, Akash V. Dixit, Tanay Roy, Srivatsan Chakram, Kevin He, Ravi K. Naik, David I. Schuster, and Aaron Chou, Stimulated emission of signal photons from dark matter waves, Phys. Rev. Lett. **132**, 140801 (2024).
[36] Hasan Padamsee, 50 years of success for SRF accelerators—a review, Supercond. Sci. Technol. **30**, 053003 (2017).
[37] Raphael Cervantes, Caterina Braggio, Bianca Giaccone, Daniil Frolov, Anna Grassellino, Roni Harnik, Oleksandr Melnychuk, Roman Pilipenko, Sam Posen, and Alexander Romanenko, Deepest sensitivity to wavelike dark photon dark matter with SRF cavities, arXiv:2208.03183.
[38] A. Romanenko *et al.*, Search for dark photons with superconducting radio frequency cavities, Phys. Rev. Lett. **130**, 261801 (2023).
[39] See Supplemental Material at http://link.aps.org/supplemental/10.1103/PhysRevLett.133.021005 for detailed description, which includes Refs. [40–47].
[40] B. Aune *et al.*, The superconducting TESLA cavities, Phys. Rev. ST Accel. Beams **3**, 092001 (2000).
[41] A. Romanenko and D. I. Schuster, Understanding quality factor degradation in superconducting niobium cavities at low microwave field amplitudes, Phys. Rev. Lett. **119**, 264801 (2017).
[42] O. Melnychuk, A. Grassellino, and A. Romanenko, Error analysis for intrinsic quality factor measurement in superconductingradio frequency resonators, Rev. Sci. Instrum. **85**, 124705 (2014).
[43] Michael S. Turner, Periodic signatures for the detection of cosmic axions, Phys. Rev. D **42**, 3572 (1990).
[44] Thomas Lacroix, Arturo Núñez Castiñeyra, Martin Stref, Julien Lavalle, and Emmanuel Nezri, Predicting the dark

matter velocity distribution in galactic structures: Tests against hydrodynamic cosmological simulations, J. Cosmol. Astropart. Phys. 10 (2020) 031.
[45] B. M. Brubaker, L. Zhong, S. K. Lamoreaux, K. W. Lehnert, and K. A. van Bibber, HAYSTAC axion search analysis procedure, Phys. Rev. D **96**, 123008 (2017).
[46] R. Cervantes *et al.*, ADMX-Orpheus first search for 70 μeV dark photon dark matter: Detailed design, operations, and analysis, Phys. Rev. D **106**, 102002 (2022).
[47] Huai-Ke Guo, Keith Riles, Feng-Wei Yang, and Yue Zhao, Searching for dark photon dark matter in LIGO O1 data, Commun. Phys. **2**, 155 (2019).
[48] R. H. Dicke, The measurement of thermal radiation at microwave frequencies, Rev. Sci. Instrum. **17**, 268 (1946).
[49] Yuriy Pischalnikov, Evgueni Borissov, Ivan Gonin, Jeremiah Holzbauer, Timergali Khabiboulline, Warren Schappert, Samuel Smith, and Jae-Chul Yun, Design and test of the compact tuner for narrow bandwidth SRF cavities, in *Proceedings of the 6th International Particle Accelerator Conference* (JACoW, Geneva, Switzerland, 2015), p. WEPTY035, 10.18429/JACoW-IPAC2015-WEPTY035.
[50] Y. Pischalnikov, D. Bice, A. Grassellino, T. Khabiboulline, O. Melnychuk, R. Pilipenko, S. Posen, O. Pronichev, and A. Romanenko, Operation of an SRF Cavity Tuner Submerged into Liquid Helium (JACoW, Geneva, Switzerland, 2019), 10.18429/JACoW-SRF2019-TUP085.
[51] Zheng-Hui Mi *et al.*, Design and test of frequency tuner for CAEP high power THz free-electron laser, Chin. Phys. C **39**, 028102 (2015).
[52] Na Liu, Yi Sun, Guang-Wei Wang, Zheng-Hui Mi, Hai-Ying Lin, Qun-Yao Wang, Rong Liu, and Xin-Peng Ma, Tuner control system of Spoke012 SRF cavity for C-ADS injector I, Chin. Phys. C **40**, 097001 (2016).
[53] Dejun Zhou *et al.*, Vertical test system for superconducting RF cavities at peking university, in *Proceedings of the 18th International Conference on RF Superconductivity* (2018), p. TUPB099, 10.18429/JACoW-SRF2017-TUPB099.
[54] Xinying Zhang *et al.*, The mechanical design, fabrication and tests of dressed 650 MHz 2-cell superconducting cavities for CEPC, Nucl. Instrum. Methods Phys. Res., Sect. A **1031**, 166590 (2022).
[55] Zhitao Yang, Jiankui Hao, Shengwen Quan, Lin Lin, Fang Wang, Fei Jiao, and Kexin Liu, Effective medium temperature baking of 1.3 Ghz single cell SRF cavities, Physica (Amsterdam) **599C**, 1354092 (2022).
[56] Gai Wang, Shengwen Quan, Lin Lin, Manqian Ren, Jiankui Hao, Fang Wang, Fei Jiao, Feng Zhu, Senlin Huang, Xueqing Yan, and Kun Zhu, Nb_3Sn cavities coated by tin vapor diffusion method at Peking university, Appl. Sci. **13**, 8618 (2023).
[57] Ciaran O'Hare, cajohare/axionlimits: Axionlimits, https://cajohare.github.io/AxionLimits/ (2020).
[58] Anthony J. Brady, Christina Gao, Roni Harnik, Zhen Liu, Zheshen Zhang, and Quntao Zhuang, Entangled sensor-networks for dark-matter searches, PRX Quantum **3**, 030333 (2022).
[59] Joshua W. Foster, Yonatan Kahn, Rachel Nguyen, Nicholas L. Rodd, and Benjamin R. Safdi, Dark matter interferometry, Phys. Rev. D **103**, 076018 (2021).
[60] Yifan Chen, Min Jiang, Jing Shu, Xiao Xue, and Yanjie Zeng, Dissecting axion and dark photon with a network of vector sensors, Phys. Rev. Res. **4**, 033080 (2022).